

Hydrazone Derivatives, an Efficient Class of Crystalline Materials for Nonlinear Optics

Christophe Serbutoviez,[†] Christian Bosshard,^{*,†} Georg Knöpfle,[†] Peter Wyss,[‡] Philippe Prêtre,[‡] Peter Günter,[‡] Kurt Schenk,[‡] Euro Solari,[§] and Gervais Chapuis[‡]

Nonlinear Optics Laboratory, Institute of Quantum Electronics, Swiss Federal Institute of Technology, ETH Hönggerberg, CH-8093 Zürich, Switzerland; Institut de Cristallographie, Université de Lausanne, Bâtiment des Sciences Physiques, Dorigny, CH-1015 Lausanne, Switzerland; and Institut de Chimie Minérale, Université de Lausanne, Bâtiment de Chimie, Dorigny, CH-1015 Lausanne, Switzerland

Received November 29, 1994. Revised Manuscript Received March 27, 1995[®]

We report on the synthesis and optical characterization of hydrazone derivatives developed for second-order nonlinear optics. Electric-field-induced second harmonic generation (EFISH) as well as semiempirical quantum-chemical computations have been carried out to investigate and explain the nonlinear optical properties of these molecules. We obtained values of up to $220 \times 10^{-40} \text{ m}^4/\text{V}$ for the molecular hyperpolarizability β at $\lambda = 1907 \text{ nm}$. The investigation of a series of 39 hydrazone derivatives with the second harmonic generation powder test according to Kurtz and Perry revealed that an extraordinarily large fraction of these hydrazones show efficient second-order nonlinear activity. Among them, 4-(dimethylamino)-benzaldehyde-4-nitrophenylhydrazone (DANPH) and 4-(1-azacycloheptyl)-benzaldehyde-4-nitrophenylhydrazone (ACNPH) were selected for more detailed investigations. Their crystalline structures are presented, and the role played by hydrogen bonds in their molecular packing is emphasized. Finally, preliminary linear and nonlinear optical data of DANPH crystals are reported.

1. Introduction

There is currently a considerable effort to develop new organic materials with large second-order nonlinear optical susceptibilities because of their potential applications in optical signal processing and frequency conversion.^{1–5} For nonlinear optical materials with large second-order nonlinearities noncentrosymmetry at both the molecular and the macroscopic level is a prerequisite for nonvanishing molecular hyperpolarizabilities β and macroscopic susceptibilities $\chi^{(2)}$. Among the various classes of materials presently investigated, organic crystals play a major role since a reliable and a time constant orientation of a hyperpolarizable chromophore in the lattice can be imposed. To date, organic crystals that have been developed for applications in nonlinear optics are built from donor–acceptor conjugated molecules. Typical examples are derivatives of 4-nitroaniline or 2-amino-5-nitropyridine.^{6–8} Since it is well established that the extension of the conjugation path (transmitter) between the electron-donating and

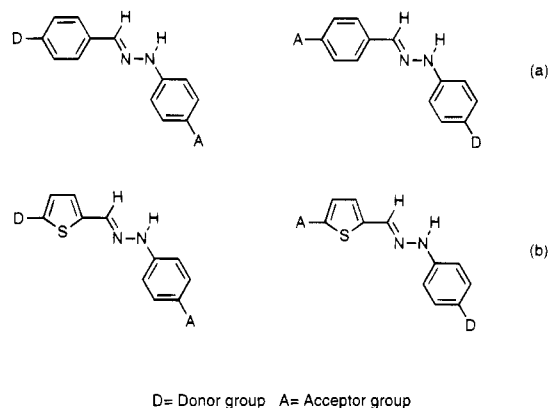


Figure 1. Push–pull derivatives of (a) benzaldehyde phenyl hydrazone and (b) thiophene-carboxaldehyde phenyl hydrazone.

–withdrawing groups strongly increases the molecular nonlinearity β ,⁹ we have prepared various organic substances based on push–pull derivatives of benzaldehyde phenylhydrazone and thiophenecarboxaldehyde phenylhydrazone (Figure 1).

Since the hydrazone backbone is an asymmetric transmitter it allows, for a given donor and acceptor group, the preparation of two different types of com-

[†] Swiss Federal Institute of Technology.

[‡] Institut de Cristallographie.

[§] Institut de Chimie Minérale.

* To whom correspondence should be addressed.

[®] Abstract published in *Advance ACS Abstracts*, May 1, 1995.

(1) Bosshard, C.; Sutter, K.; Prêtre, P.; Hulliger, J.; Flörshheimer, M.; Kaatz, P.; Günter, P. *Organic Nonlinear Optical Materials*; Gordon and Breach Science Publishers: Amsterdam, 1995.

(2) *Molecular Nonlinear Optics: Materials, Physics, Devices*; Zyss, J., Ed.; Academic Press: Boston, 1994.

(3) Prasad, P. N.; Williams, J. D. *Introduction to Nonlinear Optical Effects in Molecules and Polymers*; John Wiley and Sons, Inc.: New York, 1990.

(4) *Nonlinear Optical Properties of Organic Molecules and Crystals*; Chemla, D. S., Zyss, J., Eds.; Academic Press, Inc.: Orlando, FL, 1987.

(5) Bosshard, C.; Sutter, K.; Schlessler, R.; Günter, P. *J. Opt. Soc. Am.* **1993**, *B10*, 867.

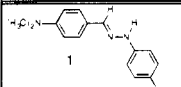
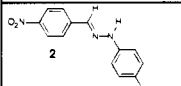
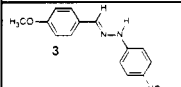
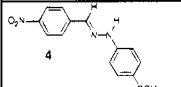
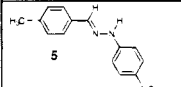
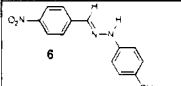
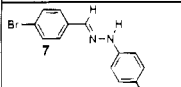
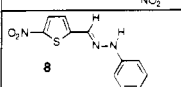
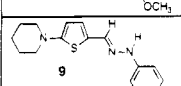
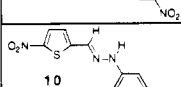
(6) Zyss, J.; Nicoud, J. F.; Coquillay, M. *J. Chem. Phys.* **1984**, *81*, 4160.

(7) Bosshard, C.; Sutter, K.; Günter, P., *J. Opt. Soc. Am.* **1989**, *B6*, 721–725.

(8) Nicoud, J. F.; Twieg, R. J. Design and Synthesis of Organic Molecular Compounds for Efficient Second-Harmonic Generation. In *Nonlinear Optical Properties of Organic Molecules and Crystals*; Chemla, D. S., Zyss, J., Eds.; Academic Press, Inc.: Orlando, FL, 1987; Vol. I, pp 227–296.

(9) Williams, D. J. *Angew. Chem.* **1984**, *98*, 637–651.

Table 2. Measured (in 1,4-Dioxane) and Extrapolated Hyperpolarizability β and β_0 in Units of $10^{-40} \text{ m}^4/\text{V}$ (Maximum of Absorption (λ_{max}) in 1,4-Dioxane and Calculated Values of μ_g)

Molecule	λ_{max} (nm)	μ_g (10^{-29} Cm)	β	β_0
	420	2.9	200	153
	464	2.6	unstable in solution	
	399	2.3	130	103
	433	2.1	160	121
	395	2.6	70	56
	423	2.3	85	65
	391	2.2	80	64
	482	2.0	220	153
	441	2.9	220	164
	470	2.4	140	100

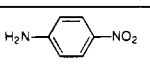
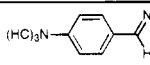
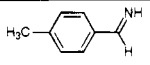
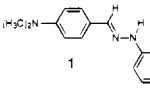
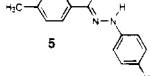
5-(1-Azacyclohexyl)-2-thiophenecarboxaldehyde-4-nitrophenylhydrazone (9): yield 90%, deep brown platelets. ^1H (NMR 200 MHz, CDCl_3) δ 1.7 (m, 6 H), 3.25 (t, $J = 6$ Hz, 4 H), 5.95 (d, $J = 4$ Hz, 1 H), 6.9 (d, $J = 4$ Hz, 1 H), 7 (d, $J = 8$ Hz, 2 H), 7.75 (s, 1 H), 7.8 (s, 1 H), 8.15 (d, $J = 8$ Hz, 2 H). Mp 186.2 °C. Anal. Calcd for $\text{C}_{16}\text{H}_{18}\text{N}_4\text{O}_2\text{S}$: C, 58.16; H, 5.49; N, 16.96; S, 9.70. Found: C, 58.18; H, 5.61; N, 16.90; S, 9.88. λ_{max} (dioxane) = 441 nm; $\epsilon = 41\,000 \text{ M}^{-1} \text{ cm}^{-1}$.

5-Nitro-2-thiophenecarboxaldehyde-4-methylphenylhydrazone (10): yield 86%, violet needles and black cubic crystals. ^1H (NMR 200 MHz, CDCl_3) δ 2.3 (s, 3 H), 6.9 (d, $J = 4$ Hz, 1 H), 7.05 (d, $J = 8$ Hz, 2 H), 7.15 (d, $J = 8$ Hz, 2 H), 7.7 (s, 1 H), 7.80 (d, $J = 4$ Hz, 1 H), 7.95 (s, 1 H). Mp 155.8 °C. Anal. Calcd for $\text{C}_{12}\text{H}_{11}\text{N}_3\text{O}_2\text{S}$: C, 55.16; H, 4.24; N, 16.08. Found: C, 55.24; H, 4.24; N, 16.14. λ_{max} (dioxane) = 470 nm; $\epsilon = 32\,000 \text{ M}^{-1} \text{ cm}^{-1}$.

4-(1-Azacycloheptyl)benzaldehyde-4-nitrophenylhydrazone (ACNPH) (12): yield 92%, red platelets. ^1H (NMR 200 MHz, CDCl_3) δ 1.6 (m, 4 H), 1.8 (m, 4 H), 3.5 (t, $J = 5$ Hz, 4 H), 6.7 (d, $J = 9$ Hz, 2 H), 7.05 (d, $J = 9$ Hz, 2 H), 7.55 (d, $J = 9$ Hz, 2 H), 7.7 (s, 1 H), 7.85 (s, 1 H), 8.15 (d, $J = 9$ Hz, 2 H). Mp 233.8 °C. Anal. Calcd for $\text{C}_{19}\text{H}_{22}\text{N}_4\text{O}_2$: C, 67.44; H, 6.55; N, 16.56. Found: C, 67.61; H, 6.37; N, 16.46. λ_{max} (dioxane) = 430 nm; $\epsilon = 40\,000 \text{ M}^{-1} \text{ cm}^{-1}$.

5-Chloro-2-thiophenecarboxaldehyde-4-nitrophenylhydrazone (13): yield 86%, deep red needles. ^1H (NMR 200 MHz, CDCl_3) δ 6.87 (d, $J = 4$ Hz, 1 H), 6.95 (d, $J = 4$ Hz, 1 H), 7.1 (d, $J = 10$ Hz, 2 H), 7.75 (s, 1 H), 7.95 (s, 1 H), 8.2 (d, $J = 10$ Hz, 2 H). Mp 145 °C. Anal. Calcd for $\text{C}_{11}\text{H}_8\text{ClN}_3\text{O}_2\text{S}$: C,

Table 3. Calculated Values of the Molecular Hyperpolarizability along the Dipole Moment and along the z Direction of Hydrazone Derivatives 1 and 5, of the 4-Nitroaniline (18), of (*E*)-4-(Dimethylamino)benzenemethanimine (19), and (*E*)-4-Methylbenzenemethanimine (20)^a

Molecule	μ_g (10^{-29} Cm)	β_z ($10^{-40} \text{ m}^4/\text{V}$)	β_{zzz} ($10^{-40} \text{ m}^4/\text{V}$)
	2.5	23	46
	0.8	25	60
	0.4	2	17
	2.9	102	172
	2.6	50	77

^a The hyperpolarizability values given here are the values directly obtained from MOPAC and converted to SI units. Since MOPAC uses a different convention for the definition of the hyperpolarizability these values cannot directly be compared with the results extrapolated from EFISH experiments.

46.97; H, 2.87; N, 14.95. Found: C, 46.86; H, 2.86; N, 14.83. λ_{max} (dioxane) = 421 nm; $\epsilon = 36\,000 \text{ M}^{-1} \text{ cm}^{-1}$.

5-(1-Azacyclohexyl)-2-thiophenecarboxaldehyde (14): piperidine (0.58 g, 6.8 mmol) and K_2CO_3 (1.87 g, 13.6 mmol) were added to a solution of 5-chloro-2-thiophenecarboxaldehyde (1 g, 6.8 mmol) in dimethyl sulfoxide (20 mL) under nitrogen atmosphere. The solution was stirred and heated at 140 °C for 20 h, cooled, poured into 200 mL of water, and extracted with CH_2Cl_2 , dried over MgSO_4 , and concentrated. A purification by chromatography over silica gel (CH_2Cl_2 , cyclohexane, 1:1) gave **14** (1.1 g, 81%) as a white solid, mp 95 °C. The product is pure enough for a condensation with various hydrazines. ^1H (NMR 200 MHz, CDCl_3) δ 1.7 (m, 6 H), 3.35 (t, $J = 6$ Hz, 4 H), 6.05 (d, $J = 5$ Hz, 1 H), 7.45 (d, $J = 5$ Hz, 1 H), 9.55 (s, 1 H).

4-(1-Azacycloheptyl)benzaldehyde (15): hexamethylenimine (1.6 g 16.1 mmol) and K_2CO_3 (4.44 g, 32.2 mmol) were added to a solution of 4-fluorobenzaldehyde (2 g, 16.1 mmol) in dimethyl sulfoxide (30 mL) under nitrogen atmosphere. The solution was stirred and heated at 140 °C for 15 h, cooled, poured into 200 mL of water, extracted with CH_2Cl_2 , dried over MgSO_4 , and concentrated. A purification by chromatography over silica gel (CH_2Cl_2 , cyclohexane, 1:1) gave **15** (2.8 g, 85%) as an oil. The product is pure enough for a condensation with various hydrazines. ^1H (NMR 200 MHz, CDCl_3) δ 1.55 (m, 4 H), 1.75 (m, 4H), 3.5 (t, $J = 6$ Hz, 4 H), 6.7 (d, $J = 10$ Hz, 2 H), 7.7 (d, $J = 10$ Hz, 2 H), 9.7 (s, 1H).

Registry Numbers: **1**, 3155-30-4; **2**, 39107-37-4; **3**, 5880-63-7; **4**, 72705-99-8; **5**, 10477-83-5; **6**, 20705-35-5; **7**, 5802-78-8; **11**, 2829-27-8; **16**, 459-57-4; **17**, 7283-96-7.

2.2. Linear Absorption Spectra. The electronic absorption spectra of push-pull hydrazone derivatives exhibit a strong transition that is highly solvatochromic.^{20,21} The behavior of the UV-vis absorption of 4-(dimethylamino)benzaldehyde-4-nitrophenylhydrazone (**1**) in various polar and nonpolar solvents is shown in Figure 4. A shift of more than

(20) Liptay, W. *Angew. Chem., Int. Ed. Engl.* **1969**, *8*, 177-188.

(21) McRae, E. G. *J. Phys. Chem.* **1957**, *61*, 562-572.

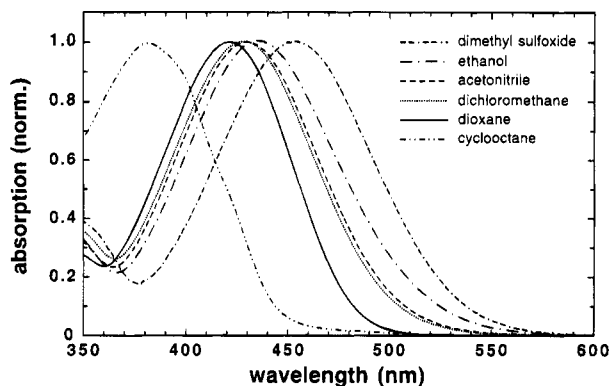


Figure 4. Shift of the wavelength of maximum absorption of DANPH in different solvents.

70 nm could be observed which proves the charge-transfer character of this transition and the potential interest of these derivatives for elaboration of new materials for second-order nonlinear optics. The transition dipole moment μ_{eg} of the molecules 1–6 was estimated by monitoring their UV–vis spectrum in dioxane and by integrating the area under their absorption band according to

$$\int_{\text{band}} \epsilon d\omega = \frac{2\pi^2 \omega_{eg}^s N_A (n^2 + 2)^2}{27 (\ln 10) \epsilon_0 c h n} \mu_{eg}^2 \quad (1)$$

where ω_{eg} is the angular transition frequency in the solvent, N_A is Avogadro's number, ϵ_0 is the vacuum permittivity, c is the speed of light, h is Planck's constant, n is the refractive index of the solvent, and ϵ is the molar extinction coefficient of the molecule.²² From the value of μ_{eg} the oscillator strength f can be calculated using²³

$$f = (2m\omega_{eg}/e^2\hbar)\mu_{eg}^2 \quad (2)$$

m is the electron mass and $\hbar = h/2\pi$. Table 1 lists the molar extinction coefficients, the transition dipole moments, and the oscillator strengths of push–pull 1,3-diphenylhydrazones. The ϵ_{max} of all molecules of type I are higher than those of the corresponding molecules of type II, but for a given couple of donor and acceptor groups the transition dipole moments associated with these electronic transitions are nearly equal. Since it is well-known that the value of an oscillator strength cannot be superior to one, it can be deduced that in hydrazone derivatives of type I and II, the highly solvatochromic band observed in UV–visible spectra (Figure 4) is in fact the result of a combination of more than one electronic transition and therefore more than one electron is involved in the charge transfer of these molecules. This result was expected due to the presence of two donor groups (D and D') which can be potentially involved in the charge transfer. This means that the central amino group of the hydrazone backbone contributes to a noticeable extent to the value of the oscillator strength in this class of molecules.

2.3. Molecular Hyperpolarizabilities. The molecular hyperpolarizabilities of the compounds 1 and 3–10 of types I and II with different donor groups were measured using the electric-field-induced second harmonic generation (EFISH) technique at 1.907 μm .²⁴ 1,4-Dioxane was used as a solvent, and the β values were calibrated against a reference solution of 2-methyl-4-nitroaniline (MNA). The hyperpolarizability β of MNA was taken as $\beta_{\text{MNA}} = 77 \times 10^{-40} \text{ m}^4/\text{V}$ ²² as determined by an EFISH experiment with crystalline quartz ($d_{11} = 0.4 \text{ pm}/\text{V}$) as a reference. A detailed description of the experimental setup and the data analysis (including the conventions used

for the definition of the hyperpolarizability and the electric field) was presented elsewhere.²² For the evaluation of the experimental data the infinite-dilution procedure as introduced by Singer and Garito²⁵ was applied. As is usually done in the EFISH technique, the contribution of the second-order hyperpolarizability $\gamma(-2\omega, \omega, \omega, 0)$ to the observed nonlinearity was neglected. Note that for extended conjugated systems this proceeding may lead to an overestimation of β of typically about 10%.²⁶ The molecular ground state dipole moments used for the evaluation of the EFISH experiments were calculated by modeling the conformation of the molecules in the gas phase and by computing the atomic charges with the semiempirical quantum-chemical program MOPAC 6 using the AM1 parametrization (see Table 2).²⁷ Since calculated dipole moments generally tend to be slightly larger than experimentally obtained values, our results for the hyperpolarizability become correspondingly smaller than if the dipole moments had been measured.

According to the quantum-mechanical two-level model the first-order molecular hyperpolarizability is given by^{28,29}

$$\beta_{CT} = \frac{3}{2\epsilon_0 \hbar^2} \frac{\omega_{eg}^2}{(\omega_{eg}^2 - 4\omega^2)(\omega_{eg}^2 - \omega^2)} \Delta\mu \mu_{eg}^2 = \frac{\omega_{eg}^4}{(\omega_{eg}^2 - 4\omega^2)(\omega_{eg}^2 - \omega^2)} \beta_0 \quad (3)$$

where $\Delta\mu = \mu_e - \mu_g$ is the difference between the excited-state and the ground-state dipole moment, μ_{eg} is the transition dipole moment between the ground state and the excited state, and ω_{eg} is the transition frequency. β_{CT} can also be expressed in terms of β_0 , the molecular hyperpolarizability extrapolated to infinite wavelengths. Table 2 lists the measured and extrapolated hyperpolarizabilities β and β_0 . Values of β_0 of up to $164 \times 10^{-40} \text{ m}^4/\text{V}$ were measured. This value is similar in size to the value reported for 4-(dimethylamino)-4-nitrostilbene (DANS), a molecule widely used in electrooptic polymers.³⁰ However, the measured values of β extrapolated to infinite wavelengths might have been biased by the two-level model which has been designed for simple systems where only one electron is involved in the charge transfer. Nevertheless the EFISH values of β at 1.907 μm (far from the absorption of our molecules) clearly indicate the high potential of hydrazones derivatives for applications in nonlinear optics.

From our EFISH measurements at 1.907 μm , the following ranking of efficiency of donor groups of benzaldehyde 4-nitrophenylhydrazone derivatives (type I) can be established:



This order is comparable to the ranking in strength of the same donor groups for push–pull nitrotolane and nitrostilbene derivatives.^{31,32}

To characterize the charge transfer associated with the hydrazone derivatives of type I, we used the semiempirical quantum chemical program package MOPAC6 to calculate the hyperpolarizabilities of selected hydrazone derivatives (hydrazones 1 and 5) and related molecules. For all molecules a gas-phase geometry optimization was performed using the AM1 parametrization of MOPAC which was also used for the hyperpolarizability calculation. The calculated hyperpolariz-

(25) Singer, K. D.; Garito, A. F. *J. Chem. Phys.* **1981**, *75*, 3572–3580.

(26) Cheng, L. T.; Tam, W.; Marder, S. R.; Stiegman, A. E.; Rikken, G.; Spangler, C. W. *J. Phys. Chem.* **1991**, *95*, 10643–10653.

(27) Dewar, M. J. S.; Zoebisch, E. G.; Healy, E. F.; Stewart, J. P. *J. Am. Chem. Soc.* **1985**, *107*, 3902–3909.

(28) Oudar, J. L.; Chemla, D. S. *J. Chem. Phys.* **1977**, *66*, 2664–2668.

(29) Lalama, S. J.; Garito, A. F. *Phys. Rev.* **1979**, *A20*, 1179–1194.

(30) Cheng, L. T.; Tam, W.; Stevenson, S. H.; Meredith, G. R.; Rikken, G.; Marder, S. J. *J. Phys. Chem.* **1991**, *95*, 10631–10643.

(31) Barzoukas, M.; Fort, A.; Klein, G.; Boeglin, A.; Serbutoviez, C.; Oswald, L.; Nicoud, J. F. *J. Chem. Phys.* **1991**, *153*, 457.

(32) Barzoukas, M.; Fort, A.; Klein, G.; Serbutoviez, C.; Oswald, L.; Nicoud, J. F. *J. Chem. Phys.* **1992**, *164*, 395.

(22) Bosshard, C.; Knöpfle, G.; Prêtre, P.; Günter, P. *J. Appl. Phys.* **1992**, *71*, 1594–1605.

(23) Oudar, J. L. *J. Chem. Phys.* **1977**, *67*, 446–457.

(24) Levine, B. F.; Bethea, C. G. *J. Chem. Phys.* **1975**, *63*, 2666–2682.

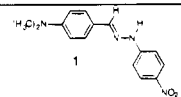
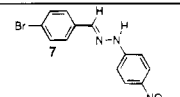
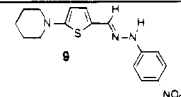
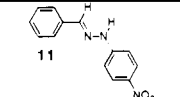
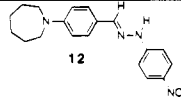
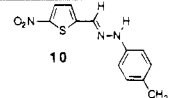
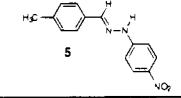
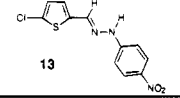
abilities of the hydrazones **1** and **5** were then compared with the equally calculated hyperpolarizabilities of 4-nitroaniline (**18**), 4-(dimethylamino)benzenemethanimine (**19**), and 4-methylbenzenemethanimine (**20**) which represent the D-A' and D'-A systems which can be found in hydrazones **1** and **5**. The calculated vector parts of β along the dipole moment, β_z , as well as the largest diagonal tensor elements, β_{zzz} , are summarized in Table 3. The results clearly demonstrate that the hyperpolarizability of hydrazone derivatives of type **I**, even for a weak donor group such as the methyl group, is superior to a noticeable extent to the sum of the static hyperpolarizabilities obtained with two classic donor-acceptor systems, e.g., 4-nitroaniline (**18**) and the 4-(dimethylamino)benzenemethanimine (**19**) for compound **1** or 4-nitroaniline and the 4-methylbenzenemethanimine (**20**) for compound **5**. This means that the molecular hyperpolarizability which is involved in hydrazones of type **I** is due not to two independent charge transfers A-D' and A'-D but to a charge transfer from the donor group to the acceptor group through the hydrazone backbone. Similarly, the high β values of the type **II** hydrazone derivatives obtained by EFISH cannot be accounted for by a partial charge transfer, e.g., between the central amino group (D') and the withdrawing group (A). In conclusion the calculated and measured values of β show that the charge transfer involved in hydrazone derivatives of type **I** and **II** is extended over all π and nonbonding electrons of the hydrazone skeleton.

Since more than one electron is involved in the charge transfer in these derivatives, according to the chemical structure of the hydrazone backbone, the lone pair of electrons of the central amino group (D') has to play an important role in the molecular hyperpolarizability of these compounds. This argument is consistent with the high influence of the position of the central amino group on the molecular hyperpolarizability of such systems. For the same electron donor and acceptor groups, the β values obtained from EFISH measurements of hydrazone derivatives of type **II**, where the central amino group is close to the donor group, are superior to a noticeable extent with respect to the corresponding molecule of type **I**, where the central amino group is close to the acceptor group. In our series of molecules the highest molecular hyperpolarizability should be obtained for compound **2** which has the strongest donor group and is of type **II**. However, due to a rapid decomposition of this molecule in solution, we were unable to measure its molecular hyperpolarizability with accuracy.

According to the two level model, the variation of the dipole moment between the excited state and the ground state $\Delta\mu$ is one of the parameters which influences the molecular hyperpolarizability. A determination of the values of $\Delta\mu$ for molecules **1** and **3-6** has been performed by using the EFISH measurements and the two level model (Table 1). For a given couple of donor and acceptor groups the $\Delta\mu$ values of hydrazones of type **II** are not noticeably superior to the values of $\Delta\mu$ of hydrazones of type **I**. However, these evaluations of $\Delta\mu$ might suffer from the lack of precision of the two level model in these classes of derivatives. In addition, an accurate determination of β_0 of these hydrazone derivatives, using the solvatochromic method (see, e.g., ref 22), is also limited in precision due to the validity of the two level model and to the difficulty to measure the cavity radius of these molecules in solution.

It has been pointed out that the substitution of both phenyl rings of stilbene derivatives with thiophene rings strongly increases the hyperpolarizabilities β while the replacement of one of the two phenyl rings does not change β by a noticeable extent.³³ In our hydrazone derivatives we have observed that already the replacement of only one phenyl ring with a thiophene ring in both molecules of types **I** and **II** reduces the energy of the charge transfer band leading to a red shift of the maximum of absorption and to an increase of the molecular hyperpolarizabilities. This result clearly demonstrates the

Table 4. Second Harmonic Powder Tests of Kurtz and Perry at 1.3 μm ^a

Molecule	SHG powder test at 1.3 μm	Molecule	SHG powder test at 1.3 μm
	***		**
	***		**
	***		***
	**		*

^a Due to large intrinsic errors which are associated with the second harmonic powder test, the results have not been quantified and only qualitative estimations of the efficiency of these crystalline materials are given by comparison with well defined crystalline materials for second-order nonlinear optics. A single asterisk denotes a signal few times greater than that of urea, whereas ** and *** refer, respectively, to 1 order of magnitude larger (typically close to PNP) and 2 orders of magnitudes larger (typically close to DAST).

importance of thiophene moieties for the elaboration of new materials for nonlinear and electrooptics.

2.4. Crystal Structures and First Nonlinear Optical Experiments. To develop organic crystals for second-order nonlinear optics we have synthesized 39 hydrazone derivatives. Out of them, 15 have given a positive second harmonic signal in the powder test at 1.3 μm (threshold of detection: urea). This high tendency for a noncentrosymmetric packing (38%) depends strongly on the substitution on the hydrazone backbone. For example more than 62% of the derivatives obtained by condensation of 4-nitrophenylhydrazine with various aldehydes are active. Such a high proportion of active materials is not often encountered during screenings of organic crystalline powders for second-order nonlinear optics. By contrast, all the hydrazone derivatives obtained from 2,4-dinitrophenylhydrazine are inactive. Table 4 summarizes the results from second harmonic powder tests of our best compounds. In a qualitative manner, a material was considered to be interesting if the second harmonic signal was at least equal to the one of 2-(*N*-prolinol)-5-nitropyridine (PNP),^{34,35} but preferably if it was close to that of 4'-(dimethylamino)-*N*-methyl-4-stilbazolium tosylate (DAST).³⁶

From the powder test, 4-(dimethylamino)benzaldehyde-4-nitrophenylhydrazone (DANPH, molecule **1**) and 4-(1-azacycloheptyl)benzaldehyde-4-nitrophenylhydrazone (ACNPH, molecule **12**) were selected for further investigations.

2.4.1. 4-(Dimethylamino)benzaldehyde-4-nitrophenylhydrazone (DANPH). DANPH has already been reported as an efficient material for second-order nonlinear optics,⁸ but we have found that the efficiency strongly depends on the crystallization conditions. Recrystallization of DANPH in various solvents showed the existence of three crystalline phases. The first one consists of a cocrystallization of DANPH with benzene in a ratio 4 to 1 (phase **I**, space group $P2_1P2_12$ ³⁷). However, due to an unfavorable orientation of the molecules in the crystal lattice, a weak efficiency of this material was observed. The second phase (phase **II**, space group *Cc*, see below) is

(34) Twieg, R. J.; Dirk, C. W. *J. Chem. Phys.* **1986**, *85*, 3537-3543.

(35) Sutter, K.; Bosshard, C.; Wang, W. S.; Surmely, G.; Günter, P. *Appl. Phys. Lett.* **1988**, *53*, 1779-1781.

(36) Marder, S. R.; Perry, J. W.; Schaeffer, W. P. *Science* **1989**, *245*, 626-628.

(37) Brown, J. N.; Kutchan, T. M.; Rist, P. E. *Cryst. Struct. Commun.* **1980**, *9*, 17.

(33) Jen, A. K.-Y.; Rao, V. P.; Wong, K. Y.; Drost, K. J. *J. Chem. Soc., Chem. Commun.* **1993**, 90-92.

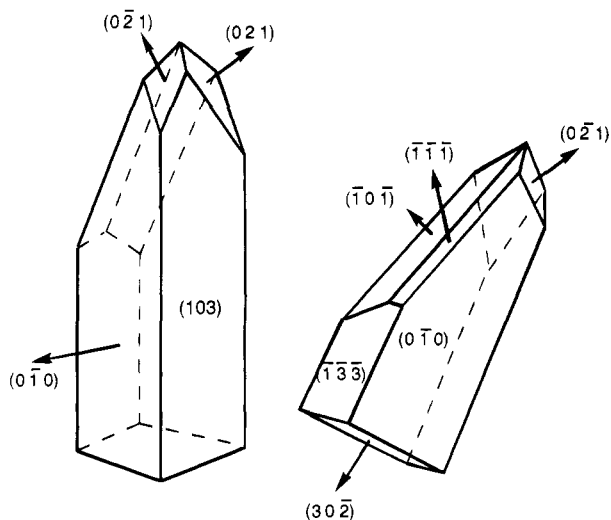


Figure 5. Typical morphology of a DANPH crystal.

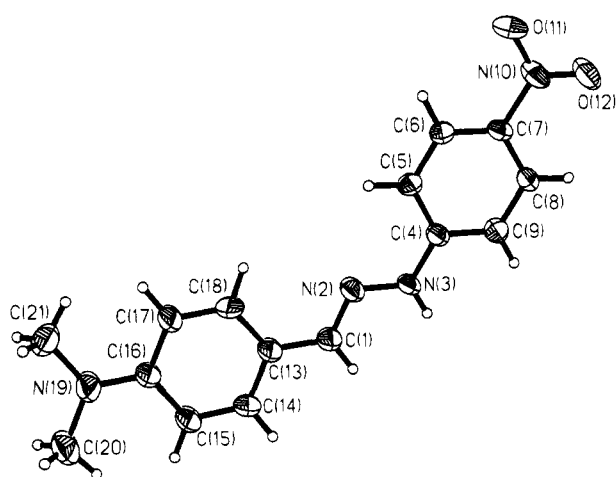


Figure 6. ORTEP drawing of DANPH (phase II).

obtained from a recrystallization in acetonitrile and consists of red greenish prisms which are highly efficient in the second-harmonic powder test at $1.3 \mu\text{m}$ and which also give a large third-harmonic signal at $1.9 \mu\text{m}$. The third phase is obtained by a slow recrystallization in ethanol and appears macroscopically as centrosymmetric, well-formed, red orange plates (phase III, space group $P2_1/c$). A heating of crystals of phase III up to 200°C for 1 min and subsequent cooling to room temperature leads to a transformation to phase II.

To study the orientation of the active chromophores in the crystalline lattice, the crystalline structures of DANPH (phase II) and ACNPH (see 2.4.2) were determined. For the data collection for DANPH a longish dark red prism had to be cut. Since no cleavage plane exists perpendicular to the needle axis, a rugged fracture plane was produced by the knife that could be indexed as $(30\bar{2})$ (Figure 5). In spite of the harsh treatment the crystal permitted an acceptable ($R_{\text{int}} = 0.049$) quick data collection. The structure was solved with the help of ShelX-TL³⁸ and the molecules (Figure 6) were refined to $R_{\text{wF}} = 0.043$ (6.4 reflections/parameter). Non-hydrogen atoms were refined anisotropically and hydrogens isotropically. The latter ones were furthermore compelled to adopt the expected geometry with C–H/N–H distances of $0.96/0.90 \text{ \AA}$.

DANPH crystallizes in point group m (space group Cc). An ORTEP plot is given in Figure 6, and its unit cell is displayed in Figure 7. The structure consists of Λ -shaped endless chains of hydrogen bonded molecules along $[101]$ (Figures 7 and 8). The hydrogen bonds are between one of the nitro oxygen atoms, O_{12} , and two hydrogen atoms, H_{1a} and H_{3a} , of the

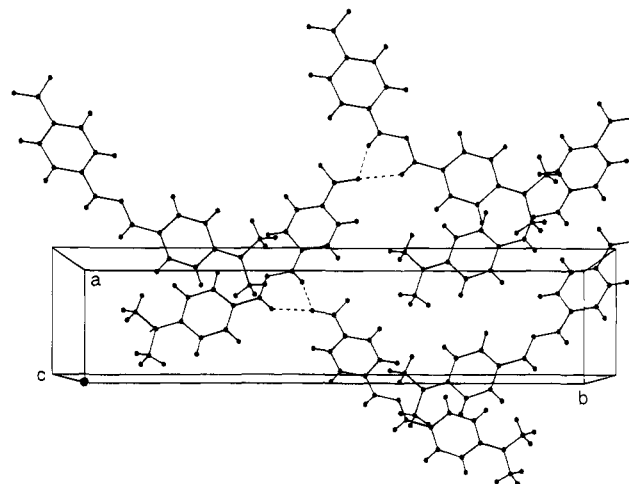


Figure 7. Drawing of DANPH phase II packing in space group Cc .

hydrazone group. The bonds are quite strong in view of the distances:

$$O_{12}-C_1: 3.37 \text{ \AA} \quad O_{12}-H_{1a}: 2.54 \text{ \AA}$$

$$O_{12}-N_3: 3.12 \text{ \AA} \quad O_{12}-H_{3a}: 2.27 \text{ \AA}$$

Tables 5 and 6 contain the structural data and the fractional coordinates for DANPH relevant for the calculation of the molecular orientation in the crystal lattice. A representation of a bulk crystal of DANPH (phase II) with Miller indices is given in Figure 5. In the crystalline structure the molecules of DANPH have a small twist angle of 11.8° between the two phenyl rings. This type of conformation is favorable for an efficient charge transfer between the electron-donor and -acceptor groups. This observation is also consistent with our conclusion that the charge transfer occurs in the entire hydrazone backbone.

The crystalline structures of DANPH (phases I and II) point out a short distance between two nitrophenyl rings of two adjacent molecules. In the case of phase II the smallest distance between the two nitrophenyl rings is equal to 3.3 \AA .

The existence of a nitrogen bond network in phase I but also in phase II avoids the formation of centrosymmetric pairs and leads to dimeric units with a lambda shape (Λ).

Since it has been shown that Λ -shaped molecules crystallize easily in noncentrosymmetric space groups, it is believed that the formation of Λ -shaped pairs in derivatives of benzaldehyde nitrophenylhydrazone by intermolecular interactions is at the origin of the high probability of finding noncentrosymmetric crystals.³⁹

Polarized vis/NIR spectra of bulk crystals of phases II and III were measured (Figures 9 and 10). Phase II of DANPH exhibits a strong absorption between 1500 and 1800 nm for light polarized parallel to the polar axis of the crystal and shows only a weak absorption in the same region when the light is polarized perpendicularly to that axis. In addition a strong anisotropy of the cutoff wavelength ($\Delta\lambda \approx 50 \text{ nm}$ at the 50% transmission point, crystal thickness of $510 \mu\text{m}$) can be observed. These results clearly indicate a strong anisotropy of this crystalline material. In contrast, the centrosymmetric form of DANPH (phase III) exhibits a polarization independent strong absorption between 1500 and 1800 nm . Note that since the cutoff of the DANPH crystals of phase II is above 650 nm , the value of the second harmonic powder test at $1.3 \mu\text{m}$ of this material may be underestimated (Table 3).

Assuming by simplicity that the charge transfer axis associated with DANPH lies between the nitrogen N(10) of the nitro group and the nitrogen N(19) of the dimethylamino group

(38) Sheldrick, G. M.; Siemens Analytical X-Ray Instruments, I. In 6300 Enterprise Lane, Madison, WI 53719-1173.

(39) Watanabe, T.; Yamamoto, H.; Hosomin, T.; Miyata, S. In *Organic Molecules for Nonlinear Optics and Photonics*; Messier, J., Ed.; Kluwer Academic: Dordrecht, 1991; Vol. 194, p 151.

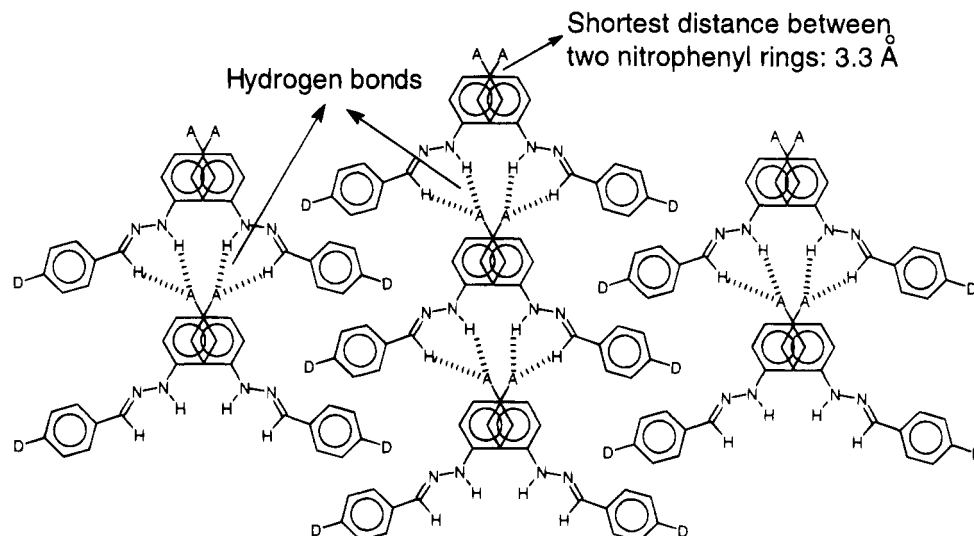


Figure 8. Schematic representation of the crystal packing of DANPH showing Λ -shaped endless chains of hydrogen bonded molecules. "A" stands for the NO_2 acceptor group and "D" stands for the $\text{N}(\text{CH}_3)_2$ donor group.

Table 5. Crystal Data for DANPH (Phase II) and ACNPH

	DANPH	ACNPH
empirical formula	$\text{C}_{15}\text{H}_{16}\text{N}_4\text{O}_2$	$\text{C}_{19}\text{H}_{22}\text{N}_4\text{O}_2$
molecular wt	284.3	338.4
color and habit	red green prisms	dark reddish platelets
crystal system	monoclinic	orthorhombic
space group	Cc	$Pca2_1$
point group	m	$mm2$
unit-cell dimensions	$a = 6.281 (2) \text{ \AA}$ $b = 28.133 (8) \text{ \AA}$ $c = 8.380 (2) \text{ \AA}$ $\beta = 97.87 (2)^\circ$	$a = 31.878 (6) \text{ \AA}$ $b = 7.1440 (10) \text{ \AA}$ $c = 7.4310 (10) \text{ \AA}$
vol	$1466.9 (4) \text{ \AA}^3$	$1692.3 (5) \text{ \AA}^3$
Z	4	4
density	1.287 g/cm^3	1.328 g/cm^3

Table 6. Final Fractional Coordinates (10^{-4}) and Equivalent Isotropic Displacement Coefficients (10^{-3} \AA^2) for DANPH^a

atom	x/a	y/b	z/c	U (eq)
N(3)	1083 (13)	4199 (2)	5649 (10)	59 (2)
C(7)	-3902 (13)	4786 (2)	7662 (9)	50 (2)
C(1)	3249 (14)	3572 (2)	5296 (10)	63 (3)
N(2)	1528	3726 (2)	5835	64 (2)
C(4)	-548 (13)	4388 (2)	6349 (10)	52 (2)
C(5)	-1871 (14)	4106 (2)	7224 (9)	60 (3)
C(13)	3894 (15)	3084 (2)	5425 (10)	67 (3)
C(9)	-928 (14)	4877 (2)	6168 (9)	56 (3)
O(12)	-5976 (12)	5436 (2)	8195 (8)	88 (2)
C(8)	-2641 (14)	5078 (2)	6848 (10)	57 (3)
O(11)	-6760 (12)	4754 (2)	9141 (8)	90 (2)
C(18)	2662 (15)	2731 (3)	5990 (12)	90 (4)
C(16)	5263 (15)	2118 (3)	5727 (10)	66 (3)
C(14)	5863 (14)	2938 (3)	5008 (11)	78 (3)
C(6)	-3527 (14)	4315 (3)	7829 (11)	64 (3)
N(10)	-5628 (14)	5009 (2)	8385 (9)	74 (3)
N(19)	5898 (14)	1657 (2)	5837 (10)	101 (4)
C(15)	6568 (16)	2471 (3)	5173 (11)	87 (3)
C(17)	3326 (16)	2261 (3)	6177 (13)	96 (4)
C(21)	4601 (18)	1304 (3)	6509 (15)	94 (4)
C(20)	8035 (19)	1511 (3)	5437 (14)	105 (4)

^a Equivalent isotropic U is defined as one-third of the trace of the orthogonalized U_{ij} tensor.

(Figure 6), the angle θ_p between the charge transfer axis and the polar axis has been estimated from crystallographic data and is equal to 52° . This means that, according to the oriented gas model,⁴⁰ the orientation of DANPH is optimized for frequency doubling. However, the orientation of the chro-

Table 7. Final Fractional Coordinates (10^{-4}) and Equivalent Isotropic Displacement Coefficients (10^{-3} \AA^2) for ACNPH^a

atom	x/a	y/b	z/c	U (eq)
C(1)	3748 (2)	-355 (9)	2901 (13)	22 (2)
N(2)	3606 (2)	1258 (8)	3323	25 (2)
N(3)	3175 (2)	1472 (8)	3119 (13)	28 (2)
C(4)	2985 (2)	3087 (10)	3625 (14)	24 (2)
C(5)	3198 (2)	4627 (9)	4281 (13)	22 (2)
C(6)	2988 (2)	6212 (10)	4823 (15)	27 (2)
C(7)	2550 (2)	6277 (9)	4655 (14)	25 (2)
C(8)	2332 (2)	4769 (10)	3962 (14)	28 (2)
C(9)	2541 (2)	3178 (9)	3458 (14)	27 (2)
N(10)	2332 (2)	7905 (9)	5268 (13)	36 (2)
O(11)	2524 (2)	9170 (6)	6062 (13)	41 (2)
O(12)	1946 (2)	7965 (8)	5010 (12)	49 (2)
C(13)	4194 (2)	-847 (9)	2898 (13)	22 (2)
C(14)	4314 (2)	-2666 (9)	2574 (13)	23 (2)
C(15)	4730 (2)	-3209 (9)	2421 (13)	20 (2)
C(16)	5050 (2)	-1845 (9)	2651 (13)	22 (2)
C(17)	4927 (2)	6 (10)	3037 (14)	22 (2)
C(18)	4508 (2)	507 (10)	3138 (13)	26 (2)
N(19)	5467 (2)	-2351 (7)	2472 (13)	21 (2)
C(20)	5583 (2)	-3981 (9)	1418 (14)	23 (2)
C(21)	5679 (2)	-5701 (9)	2554 (14)	24 (2)
C(22)	6099 (2)	-5574 (10)	3538 (14)	29 (2)
C(23)	6167 (2)	-3804 (10)	4621 (14)	29 (2)
C(24)	6214 (2)	-2047 (10)	3447 (14)	27 (2)
C(25)	5800 (2)	-1027 (10)	3002 (14)	26 (2)

^a Equivalent isotropic U is defined as one-third of the trace of the orthogonalized U_{ij} tensor.

mophores in the lattice is not optimized for electrooptics due to the Λ shape orientation of the molecules. Nevertheless, large values of the macroscopic nonlinear optical susceptibilities d_{ijk} are expected due to the high values of the molecular hyperpolarizabilities. As an example we give a rough estimate of the largest nonlinear optical coefficient d_{12} of DANPH using the measured value $\beta = 200 \times 10^{-40} \text{ m}^4/\text{V}$ at $\lambda = 1.907 \text{ \mu m}$ ($\lambda_{\text{max}} = 420 \text{ nm}$ in 1,4-dioxane), the angles between the charge transfer axis of the molecules and the dielectric axes x and y of the crystal ($\theta_{\text{CT},x} = 128^\circ$, $\theta_{\text{CT},y} = 140.2^\circ$), the number density of the molecules in the crystal $N = 2.727 \times 10^{27} \text{ m}^{-3}$, a local field correction of 10, the two-level model, and the oriented gas model.^{1,40} This simple approximation gives a value for d_{12} of around 250 pm/V at $\lambda = 1.5 \text{ \mu m}$.

2.4.2. 4-(1-azacycloheptyl)benzaldehyde-4-nitrophenylhydrazone (ACNPH). ACNPH crystals were obtained as deep red platelets from a slow recrystallization in ethanol. In contrast to DANPH no crystalline modifications could be found. However, crystal growth of ACNPH seems to be problematic since

(40) Zyss, J.; Oudar, J. L. *Phys. Rev.* **1982**, *A26*, 2028-2048.

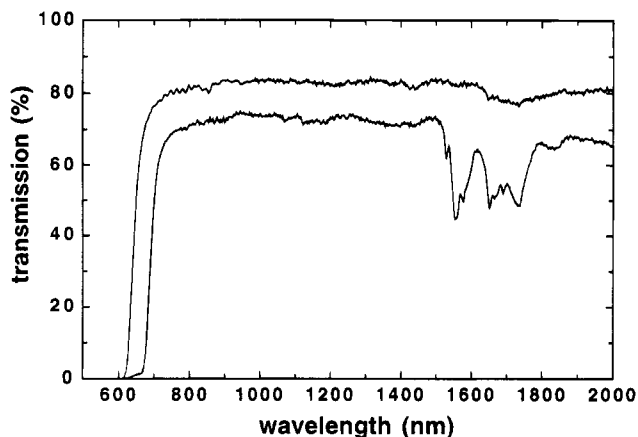


Figure 9. Transmission spectrum of DANPH (phase II) for the incident light polarized parallel to the polar axis of the crystal (upper curve) and for light polarized perpendicularly to that axis (lower curve). An as grown unpolished crystal was used (crystal thickness of 510 μm).

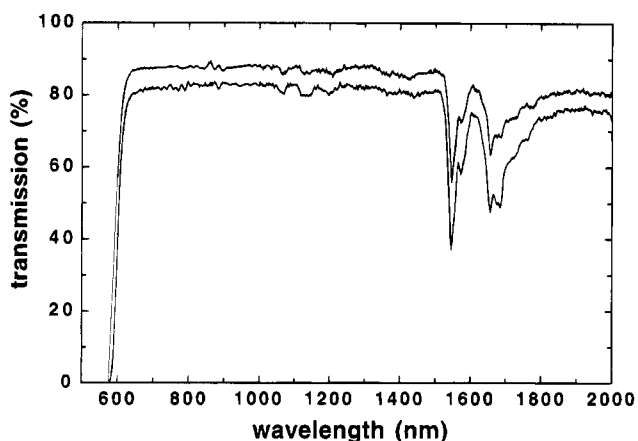


Figure 10. Transmission spectrum of DANPH (phase III) for the incident light polarized parallel to the main axes of the crystal. An as grown unpolished crystal was used (crystal thickness of 1 mm).

suitable crystals for X-ray diffraction can be obtained only by the gel growth technique.⁴¹

A rather well-developed {100} platelet was used for the collection of X-ray intensities. It was glued to the rim of a glass capillary and kept at a temperature of 130 K. The structure was solved by means of ShelXTL,³⁸ and the molecules (Figure 11) refined to $R_{\text{wF}} = 0.052$ (4.7 reflections per parameter). Non-hydrogen atoms were refined anisotropically and hydrogens isotropically. The latter ones were furthermore forced to adopt the expected geometry with C-H/N-H distances of 0.96/0.90 Å.

ACNPH crystallizes in point group $mm2$ (space group $Pca2_1$). The structure consists of Λ -like endless chains of hydrogen-bonded molecules along $[\bar{1}01]$, and another such chain along $[101]$ (Figure 12). The hydrogen bonds are between the two nitro oxygen atoms O_{11} and O_{12} , and the two hydrogen atoms, H_{1a} and H_{3a} , of the hydrazone group, as well as one hydrogen atom of the phenyl ring, H_{9a} . The bonds are quite strong in view of the distances:

$$\begin{array}{ll} O_{12}-C_1: 3.31 \text{ \AA} & O_{12}-H_{1a}: 2.52 \text{ \AA} \\ O_{11}-N_3: 3.16 \text{ \AA} & O_{11}-H_{3a}: 2.32 \text{ \AA} \end{array}$$

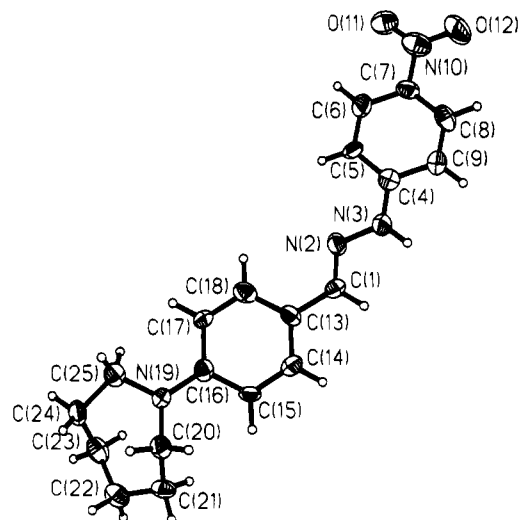


Figure 11. ORTEP drawing of ACNPH.

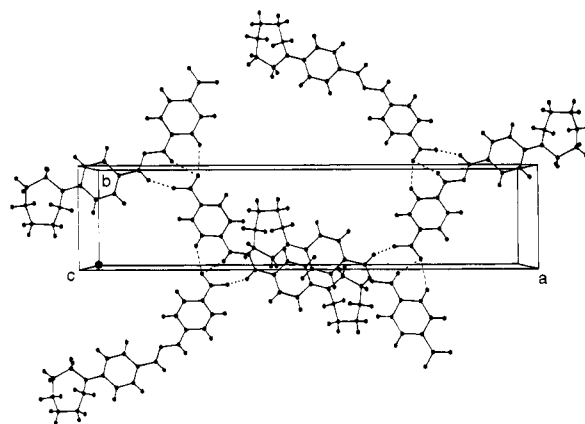


Figure 12. Drawing of ACNPH packing in space group $Pca2_1$.

$$O_{11}-C_9: 3.38 \text{ \AA} \quad O_{11}-H_{9a}: 2.57 \text{ \AA}$$

Tables 5 and 7 contain the structural data and the fractional coordinates for ACNPH. An ORTEP plot of ACNPH is given in Figure 11, and the unit cell is shown in Figure 12. As in the case of DANPH, the molecules in the crystal have a twist angle of 11.8° between their two phenyl rings which is favorable for an efficient charge transfer between the donor and acceptor group.

Interestingly, also the hydrogen bond network between the central amino of a hydrazone backbone and the terminal nitro groups of two other hydrazone molecules is present just as in DANPH. As has been explained above this combination of intermolecular interactions between molecules limits the formation of centrosymmetric pairs and leads to dimeric units with a Λ -shape.

Assuming by simplicity that the charge transfer axis associated with ACNPH lies between the nitrogen N(10) of the nitro group and the nitrogen N(19) of the acycloheptyl group (Figure 11), the angle θ_p between the charge transfer axis and the polar axis has been estimated from crystallographic data and is equal to 80° . Therefore, according to the oriented gas model, the orientation of ACNPH is unfavorable for second-order nonlinear optics.⁴⁰

3. Discussion and Conclusion

The application of organic materials for second-order nonlinear optics can be divided into three areas: materials for electrooptics, materials for frequency doubling and parametric amplification, and materials for photorefractive applications. Due to the natural tendency of derivatives of benzaldehyde nitrophenylhydrazones to

(41) Arend, H.; Connelly, J. J. *J. Cryst. Growth* **1982**, *56*, 642.

crystallize in Λ -shaped pairs, it seems difficult to have a crystalline packing optimized for electrooptics where all the molecules are parallel to each other. The application of the presented materials for frequency doubling into the blue or green spectral range on the other hand is prevented by the relatively large absorption wavelengths. However, due to the donating character of the hydrazone backbone, it is conceivable to obtain materials for frequency doubling by replacing the donating group and the acceptor group of hydrazones of type **I** and **II** with weak withdrawing groups. If the formation of Λ -shaped pairs is remained, it should be possible to obtain colorless and optimized crystalline materials for frequency conversion even into the blue spectral region. A similar methodology, but transposed to chalcone derivatives, has already been successful in the search for materials possessing a wide transparency range in the visible region.⁴²

In conclusion, we have demonstrated the relevance of push-pull hydrazones for quadratic nonlinear optics by the measurement of the molecular hyperpolarizabilities. The molecular nonlinearity of hydrazones of type **II** is to a noticeable extent larger than the nonlinearity of the corresponding type **I** derivative. In addition we

established that thiophene moieties are very important in enhancing the molecular nonlinearity in our hydrazone derivatives. The second-order powder tests showed a high probability for noncentrosymmetric crystal packing in such materials. A bulk crystal of DANPH has already been obtained from acetonitrile. The determination of the refractive indices and of the nonlinear optical coefficients is under progress. Further work will concentrate on the determination of the crystalline structures of the other active compounds of Table 4, such as compound **10** which crystallizes nicely as black crystals. Note that the compounds described in this work are not only promising for crystals. Since the hydrazone derivatives exhibit larger ground-state dipole moments μ_g and second-order polarizabilities β than the standard dyes used in electrooptic polymers, efficient materials could also be prepared from guest-host or side-chain polymers if the thermal and the light stability of these chromophores are controlled.

Acknowledgment. This research was supported by the Swiss National Science Foundation.

Supplementary Material Available: Listing of hydrogen atom positions, bond distances, and angles (3 pages). Ordering information is given on any current masthead page.

CM940531K

(42) Fichou, D.; Watanabe, T.; Takeda, T.; Miyata, S.; Nakayama, M. *Jpn. J. Appl. Phys.* **1988**, L249, 27.